in vivo *38*: 160-173 (2024)
doi:10.21873/invivo.13422

Deletion of RAMP1 Signaling Enhances Diet-induced Obesity and Fat Absorption *via* Intestinal Lacteals in Mice

KANAKO HOSONO[1,2], ATSUSHI YAMASHITA[2], MINA TANABE[2], YOSHIYA ITO[1,2], MASATAKA MAJIMA[3], KAZUTAKE TSUJIKAWA[4] and HIDEKI AMANO[1,2]

[1]*Department of Pharmacology, Kitasato University School of Medicine, Sagamihara, Japan;*
[2]*Department of Molecular Pharmacology, Graduate School of Medical Sciences, Kitasato University, Sagamihara, Japan;*
[3]*Department of Medical Therapeutics, Kanagawa Institute of Technology, Kanagawa, Japan;*
[4]*Laboratory of Molecular and Cellular Physiology, Graduate School of Pharmaceutical Sciences, Osaka University, Osaka, Japan*

Abstract. *Background/Aim: Intestinal lymphatic vessels (lacteals) play a critical role in the absorption and transport of dietary lipids into the circulation. Calcitonin gene-related peptide and receptor activity-modifying protein 1 (RAMP1) are involved in lymphatic vessel growth. This study aimed to examine the role of RAMP1 signaling in lacteal morphology and function in response to a high-fat diet (HFD). Materials and Methods: RAMP1 deficient ($RAMP1^{-/-}$) or wild-type (WT) mice were fed a normal diet (ND) or HFD for 8 weeks. Results: $RAMP1^{-/-}$ mice fed a HFD had increased body weights compared to WT mice fed a HFD, which was associated with high levels of total cholesterol, triglycerides, and glucose. HFD-fed $RAMP1^{-/-}$ mice had shorter and wider lacteals than HFD-fed WT mice. HFD-fed $RAMP1^{-/-}$ mice had lower levels of lymphatic endothelial cell gene markers including vascular endothelial growth factor receptor 3 (VEGFR3) and lymphatic vascular growth factor VEGF-C than HFD-fed WT mice. The concentration of an absorbed lipid tracer in HFD-fed $RAMP1^{-/-}$ mice was higher than that in HFD-fed WT mice. The zipper-like continuous junctions were predominant in HFD-fed WT mice, while the button-like discontinuous junctions were predominant in HFD-fed $RAMP1^{-/-}$ mice. Conclusion: Deletion of RAMP1 signaling suppressed lacteal growth and VEGF-C/VEGFR3 expression but accelerated the uptake and transport of dietary fats through discontinuous junctions of lacteals, leading to excessive obesity. Specific activation of RAMP1 signaling may represent a target for the therapeutic management of diet-induced obesity.*

Correspondence to: Yoshiya Ito, MD, Ph.D., Department of Pharmacology, Kitasato University School of Medicine, 1-15-1 Kitasato, Minami-ku, Sagamihara, Kanagawa 252-0374, Japan. Tel: +81 427789113, Fax: +81 427788441, e-mail: yito@kitasato-u.ac.jp

Key Words: Lacteal, macrophage, RAMP1, absorption, fat.

The specialized lymphatic capillaries situated at the center of each intestinal villus are known as lacteals. Lacteals carry absorbed dietary lipids and drain them into the submucosal lymphatic networks of the intestines. Lipids are then transported to the thoracic duct through the mesenteric lymphatics (1). Considering the essential role of lacteals in intestinal lipid absorption, dysregulation of lipid transport by lacteals contributes to various adverse health conditions, including the progression of obesity, which is now prevalent worldwide. Obesity is related to systemic metabolic consequences in adults (2-4) and is a high-risk factor for cardiovascular diseases (5). Obesity is also accompanied by metabolic dysfunction-associated steatotic liver disease, which is currently the most common chronic liver disease worldwide, with a global prevalence of 25% (6). These findings indicate that the progression of obesity is related to stimulation of lymphatic transport *via* the lymphatic vessels.

Lymphangiogenesis, the formation of new lymphatic vessels from pre-existing ones, is regulated by prolymphangiogenic growth factors, including vascular endothelial growth factor (VEGF)-C and VEGF-D. Vascular endothelial growth factor receptor 3 (VEGFR3) is a receptor of VEGF-C and VEGF-D, which is expressed in lymphatic endothelial cells (ECs). The transcription factor prospero-related homeobox 1 (Prox1) is a master regulator of lymphatic development and lymphangiogenesis. Defects in the genes related to lymphatic growth or function induce abnormal adipose tissue deposition and obesity. Indeed,

experimental animal studies have shown that defective lymphatic vascular structures and lymphatic malfunction can be linked to obesity. Disorders of lymphatic vascular growth in $Prox1^{+/-}$ mice are characteristic of adult-onset obesity (7, 8). In addition, leakage from lymphatic vessels and accumulation of adipose tissue have been observed in lymphedema mice with genetic inactivation of VEGFR3 tyrosine kinase. Over-expression of VEGF-C genes restores functional lymphatic vessels in mice with lymphedema, suggesting that enhanced expression of VEGF-C stimulates the growth of functional lymphatic vessels through the activation of VEGFR3 (9). Therefore, structure and function of the intestinal lacteals are mainly maintained by VEGF-C/VEGFR3 signaling.

Recent evidence indicates that lacteal integrity is maintained by continuous signals derived from stromal cells surrounding the lacteals (10). The longitudinal smooth muscle cells (SMCs) around the lacteals generate VEGF-C to regulate lacteal integrity and lipid transport through VEGFR3 signaling in the lymphatic ECs comprising the lacteals (11). Additionally, macrophages in the intestinal villi are a source of VEGF-C, which maintains lacteal morphology and function (12).

Calcitonin gene–related peptide (CGRP), a 37-amino acid neuropeptide, innervates the gastrointestinal tract, including the stomach (13) and intestines (14, 15). In particular, $CGRP^{+}$ nerve fibers are widely distributed along the lacteals (14, 15). CGRP exerts its action through the CGRP receptor, which comprises heterodimer subunits: calcitonin receptor-like receptor (CLR) and receptor activity-modifying protein (RAMP) 1, which regulates specific CGRP binding to CLR (16, 17). We have previously shown that CGRP/RAMP1 is responsible for the development of lymphatic vessels in mice with skin wounds (18), endometriosis (19), and secondary lymphedema (20). Under these pathological conditions, CGRP/RAMP1 signaling promotes inflammation-associated lymphatic vessel formation by inducing pro-lymphangiogenic stimulating factor production derived from accumulated immune cells.

These findings led us to hypothesize that RAMP1 signaling contributes to diet-induced obesity by affecting lacteals function. Therefore, the current study was conducted to examine the role of RAMP1 signaling in lipid uptake *via* lacteals in diet-induced obese mice.

Materials and Methods

Animals. Male RAMP1-deficient ($RAMP1^{-/-}$) mice were generated as described elsewhere (21). Male C57BL/6 wild type (WT) mice were obtained from CLEA Japan (Tokyo, Japan). All mice were housed at constant humidity (50%±5%) and temperature (25˚C±1˚C) on a 12 h light/dark cycle and were given ad libitum access to water and food. All experimental protocols were reviewed and approved by the Institutional Animal Care and Use Committee (Approval no. 2022-057). The animal experimental procedures were performed in accordance with the guidelines of the Science Council of Japan for animal experiments.

Experimental protocols. Mice were fed a normal diet (ND; 344.9 kcal/100 g, fat kcal 4.6%; CLEA Japan) or high-fat diet (HFD) (56.7% kcal from fat, 32% fat powdered oil, CLEA Japan) at 4 weeks of age for a period of 8 weeks. Body weight was weekly monitored. After HFD or ND feeding, the mice were anesthetized with isoflurane (Pfizer, New York City, NY, USA), and blood was collected by cardiac puncture. Then, perirenal fat and epididymal fat were carefully removed. The small intestine was cut longitudinally and washed with phosphate-buffered saline (PBS) to remove fecal material, and the jejunum segments were excised and collected. Following this procedure, the animals were euthanized *via* cervical dislocation. Serum was used to determine the total cholesterol and triglyceride levels using a Dri-Chem 7000 Chemistry Analyzer System (Fujifilm, Tokyo, Japan). The levels of blood glucose were determined using a blood glucose meter (TERUMO Corp., Tokyo, Japan). White adipose tissue (WAT) from the epididymal and perirenal fat tissues was weighed.

Analysis of lacteal function. To analyze lymph transport *via* lacteals, mice were fasted overnight before oral administration of the fluorescent lipid tracer BODIPY FL C16 FA (Invitrogen, Carlsbad, CA, USA) (0.1 mg in 200 μl olive oil) (22). At 3 h after the oral administration of BODIPY, the mice were euthanized, and blood was collected *via* cardiac puncture. BODIPY fluorescence in the serum was measured at 470 nm using a NanoDrop 3300 (Thermo Fisher Scientific, Waltham, MA, USA), and data were normalized to the serum from mice given only olive oil. Concomitantly, the jejunum was examined using immunofluorescence analysis (Biozero BZ-700 Series; KEYENCE, Osaka, Japan).

Collection of dorsal root ganglion (DRG.) Under anesthesia with isoflurane, thoracic DRGs from the $Th_{4\text{-}12}$ vertebrae were dissected (23) and collected. The samples were prepared for quantitative PCR or immunohistochemistry analyses.

Immunohistochemical analysis. Tissue samples from the removed DRGs were fixed immediately with 4% paraformaldehyde in PBS at 4˚C overnight. Paraffin-embedded DRG sections (3.5 μm-thick) were used for immunostaining. After blocking with serum-free protein block (Dako, Glostrup, Denmark), the sections were incubated at 4˚C overnight with an anti-CGRP antibody (rabbit polyclonal antibody, 1:200; Sigma-Aldrich, St. Louis, MO, USA). Then, the sections were incubated using the Universal DAKO LSAB system HRP (Dako) with DAB and the tissues were counterstained with Mayer's hematoxylin solution.

Immunofluorescence analysis. Excised jejunum tissue samples were fixed with periodate-lysine-paraformaldehyde at 4˚C overnight. Then, the samples were transferred to 30% sucrose in 0.1 M phosphate buffer. The sections (16-μm-thick) were blocked with 1% bovine serum albumin in 0.5% Triton X-100 in PBS and incubated overnight at 4˚C with the following primary antibodies: F4/80 (rat monoclonal antibody, A3-1, 1:100; Bio-Rad Laboratories, Hercules, CA, USA), anti-mouse RAMP1 (rabbit polyclonal antibody, 1:100; Invitrogen, Carlsbad, CA, USA), and anti-mouse VEGF-C (rabbit polyclonal antibody, 1:100; Abcam, Cambridge, UK). Then, the sections were incubated with the following secondary antibodies for

Table I. *Primers used for reverse transcription and quantitative PCR.*

Gene	Forward primer sequence (5'–3')	Reverse primer sequence (5'–3')
GAPDH	ACATCAAGAAGGTGGTGAAGC	AAGGTGGAAGAGTGGGAGTTG
RAMP1	CCATCTCTTCATGGTCACTGC	AGCGTCTTCCCAATAGTCTCC
LYVE-1	GCTCTCCTCTTCTTTGGTGCT	TGACGTCATCAGCCTTCTCTT
VEGFR-3	CTCTCCAACTTCTTGCGTGTC	GCTTCCAGGTCTCCTCCTATC
Prox-1	GTTCTTTTACACCCGCTACCC	ACTCACGGAAATTGCTGAACC
VEGF-C	TCTGTGTCCAGCGTAGATGAG	GTCCCCTGTCCTGGTATTGAG
VEGF-D	CCTATTGACATGCTGTGGGAT	GTGGGTTCCTGGAGGTAAGAG
VEGF-A	ACGACAGAAGGAGAGCAGAAG	ATGTCCACCAGGGTCTCAATC
VEGFR-1	GTCTCCATCAGTGGCTCTACG	CCCGGTTCTTGTTGTATTTTG
VEGFR-2	CTGCCTACCTCACCTGTTTCC	CGGCTCTTTCGCTTACTGTTC

2 h at room temperature: Alexa Fluor 488-conjugated donkey anti-rabbit IgG and Alexa Fluor 594-conjugated donkey anti-rat IgG (all from Molecular Probes, Eugene, OR, USA). Whole-mounted jejunum tissues were fixed using 4% paraformaldehyde and then incubated for 3 d at 4˚C with the following primary antibodies: anti-mouse LYVE-1 (rabbit polyclonal antibody, 1:200; Abcam), anti-mouse LYVE-1 (goat polyclonal antibody, 1:100; BD Biosciences, Franklin Lakes, NJ, USA), anti-mouse alpha smooth muscle actin (α-SMA) (rabbit polyclonal antibody, 1:200; Abcam), anti-mouse actin, α-smooth muscle-Cy3 (mouse monoclonal antibody, 1A4, 1:200; Sigma-Aldrich), anti-mouse CGRP (rabbit polyclonal antibody, 1:100; Sigma-Aldrich), or anti-mouse vascular endothelial (VE)-cadherin (goat polyclonal antibody, 1:200; R&D systems, Minneapolis, MN, USA). Then, the sections were incubated with the following secondary antibodies at 4˚C overnight: Alexa Fluor 488-conjugated donkey anti-rabbit IgG, Alexa Fluor 488-conjugated donkey anti-goat IgG, Alexa Fluor 594-conjugated donkey anti-rabbit IgG, Alexa Fluor 594-conjugated donkey anti-goat IgG, and Alexa Fluor 647-conjugated donkey anti-rabbit IgG (all from Molecular Probes). Nuclei were detected with DAPI. The images were captured with a confocal scanning laser microscope (LSM710; Carl Zeiss, Jena, Germany) or fluorescence microscope (Biozero BZ-700 Series; KEYENCE, Osaka, Japan).

Morphometric analysis. Morphometric assessments were performed using the ImageJ software version 1.46r (National Institutes of Health, Bethesda, MD, USA). Images co-stained with α-SMA and LYVE-1, in which whole villi were visualized together with lacteals, were selected. The absolute length and width of the villi and lacteals were determined from 5–10 villi in each animal. In addition, lacteal junctions were visualized by staining with VE-cadherin. Zipper-type junctions were defined as continuous junctions at the cell–cell borders with elongated cells. Button-like junctions were defined as discontinuous junctions that were not parallel to the cell–cell borders (24).

Quantitative real-time reverse transcriptase-PCR analysis. Total RNA was extracted from the mouse tissues using RNAiso Plus (Takara Bio, Shiga, Japan). Single-stranded cDNA was generated from 1 μg total RNA by reverse transcription using a ReverTra Ace qPCR RT Kit (Toyobo, Osaka, Japan). Real-time quantitative PCR was performed using TB Green Premix Ex Taq II (Tli RNase H Plus; Takara Bio). The gene-specific primers used in these experiments are listed in Table I. mRNA expression levels were normalized to glyceraldehyde-3-phosphate dehydrogenase mRNA levels in the same sample.

Statistical analysis. All results are presented as mean±standard deviation (SD). An unpaired two-tailed Student's *t*-test was used to compare data between the two groups. Data between multiple groups were compared using one-way analyses of variance, followed by Tukey's post hoc tests. Statistical significance was set at $p<0.05$. In the graphs, significance is depicted with asterisks as follows: $*p<0.05$, $**p<0.01$, $***p<0.001$. Statistical analysis was performed using GraphPad Prism software version 8 (GraphPad Software, La Jolla, CA, USA).

Results

RAMP1 deficiency resulted in obesity. To determine the role of RAMP1 in obesity, we examined the sequential changes in the body weight of mice fed normal and high-fat diets. On a ND, the body weight was similar in both RAMP1$^{-/-}$ and WT mice. When RAMP1$^{-/-}$ mice were fed a HFD, their body weight increase was 15% higher than that of WT mice on a HFD (Figure 1A and B). During HFD feeding, the difference in HFD-induced body weight gain between WT and RAMP1$^{-/-}$ mice was significant. Consistent with acceleration of body weight gain in HFD-fed RAMP1$^{-/-}$ mice, total WAT was 26% more in HFD-fed RAMP1$^{-/-}$ mice than that in HFD-fed WT mice (Figure 1B). The concentrations of total cholesterol and triglycerides in HFD-fed RAMP1$^{-/-}$ mice were greater than those in HFD-fed WT mice (Figure 1C). The same was true for non-fasting blood glucose levels. However, no differences in these parameters were observed when feeding ND between the two phenotypes. These results indicated that HFD-induced obesity was more severe in RAMP1$^{-/-}$ mice than that in WT mice.

HFD-fed RAMP1$^{-/-}$ mice had short lacteals. Next, we examined whether HFD-induced body weight gain in RAMP1$^{-/-}$ mice was accompanied by altered lacteal structure and dysregulated lipid absorption by the intestinal

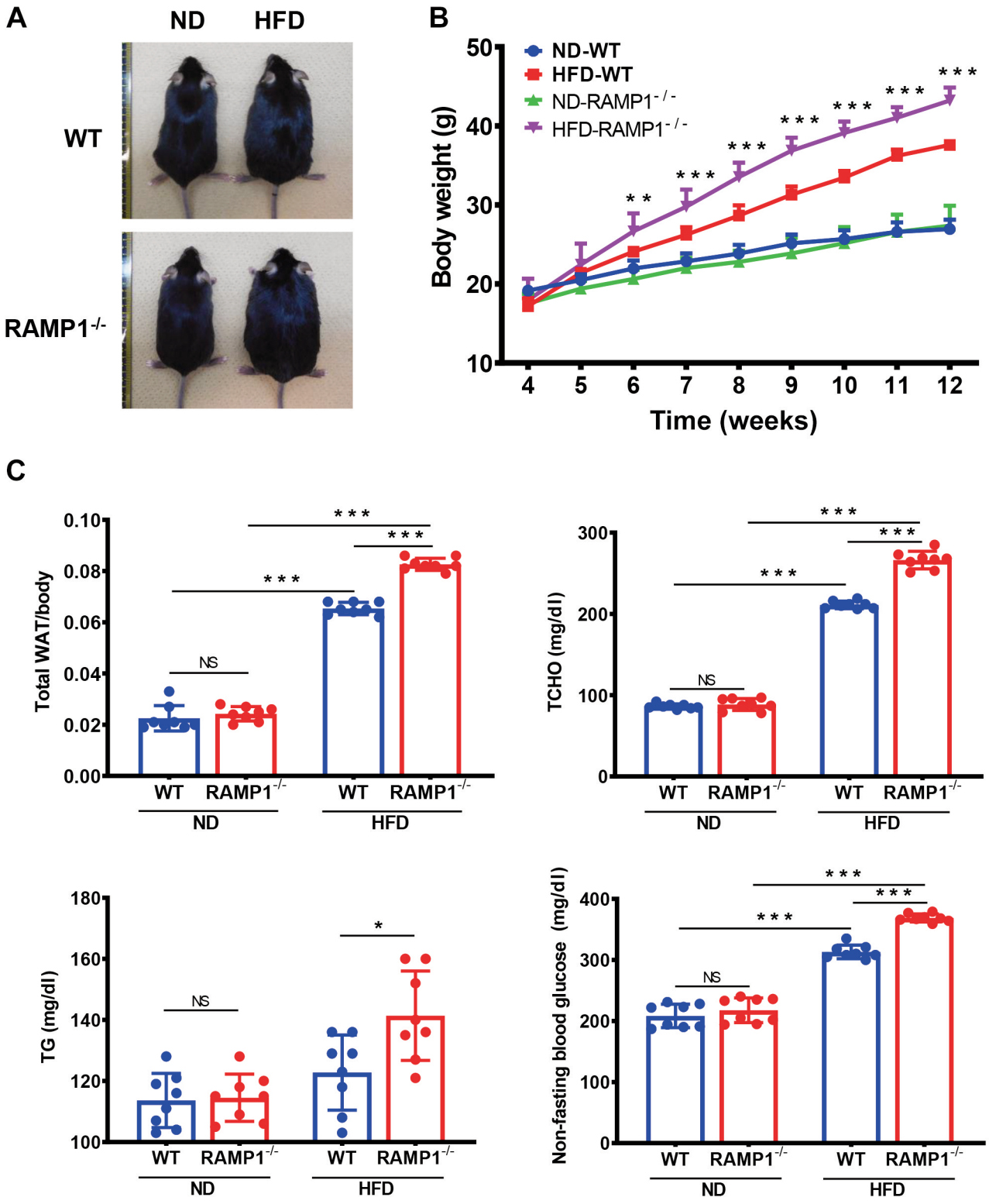

Figure 1. *Aggravated obesity and fat levels in RAMP1$^{-/-}$ mice. (A) Representative photos of the body of wild type (WT) and RAMP1$^{-/-}$ mice fed normal diet (ND) or high-fat diet (HFD) for 8 weeks. (B) Changes in the body weight of WT and RAMP1$^{-/-}$ mice after feeding ND or HFD from 4 weeks of age through 12 weeks of age. **p<0.01 vs. HFD-WT and ***p<0.001 vs. HFD-WT. (C) Total white adipose tissue (WAT)/body weight and serum levels of total cholesterol (TCHO), triglycerides (TG), and non-fasting blood glucose in WT and RAMP1$^{-/-}$ mice after feeding ND or HFD. Data are expressed as the mean±SD. *p<0.05 and ***p<0.001; NS: not significant.*

lacteals. To this end, we performed immunostaining for LYVE-1 and α-SMA in intestinal whole-mounts. Using whole-mount immunostaining, we visualized the epithelial lining, longitudinal smooth muscle cells stained with α-SMA, and lacteals stained with LYVE-1 in the villi of the jejunum (Figure 2A). Quantitative analyses revealed that the villi length and width did not differ between WT and RAMP1$^{-/-}$ mice fed ND (Figure 2B). The length of lacteals from HFD-fed RAMP1$^{-/-}$ mice was shorter than that from HFD-fed WT mice, although there was no statistically significant difference between WT and RAMP1$^{-/-}$ mice fed ND. Furthermore, the lacteals width in RAMP1$^{-/-}$ mice was greater than that in WT mice.

Expression of CGRP and RAMP1. The above results suggested that RAMP1 signaling was involved in changes in lacteal structure during HFD feeding. Therefore, the expression of CGRP and RAMP1 in the intestinal villi was examined (Figure 3A). Immunofluorescence analysis revealed that CGRP nerve fibers were abundantly distributed around the lacteals and smooth muscle fibers in WT mice. The density of CGRP nerve fibers appeared to be similar between WT and RAMP1$^{-/-}$ mice fed ND or HFD. In addition, RAMP1 in the villi colocalized with F4/80^{+} cells in the stroma of the intestinal villi (Figure 3B), suggesting that macrophages expressed RAMP1. The mRNA expression of RAMP1 in the jejunum in WT mice fed HFD did not differ from that in WT mice fed ND. As extrinsic C-sensory afferents, including CGRP^{+} nerves, arise from the DRG, the expression of CGRP in the thoracic DRG was determined (Figure 3C). The percentage of CGRP^{+} neurons increased during HFD feeding in both the genotypes. However, no statistically significant differences in the number of CGRP^{+} neurons were demonstrated between the two groups.

Downregulated expression of lymphatic EC markers and pro-lymphangiogenic factors in HFD-fed RAMP1$^{-/-}$ mice. Recent studies have shown that VEGF-C/VEGFR3 signaling contributes to the maintenance of lacteal integrity (11, 24). We determined the expression of lymphatic EC-related genes. mRNA levels of factors related to lymphatic ECs, including *Lyve-1*, *Vegfr3*, and *Prox1*, in HFD-fed WT mice were higher than those in ND-fed WT mice (Figure 4A). The mRNA levels of these factors in HFD-fed RAMP1$^{-/-}$ mice were lower than those in HFD-fed WT mice. The same was true for gene expression of *Vegfc*, a lymphangiogenic stimulating factor; however, there were no statistically significant differences in *Vegfd* mRNA expression between the groups. We further examined the source of VEGF-C in intestinal villi. Immunofluorescence analysis revealed that VEGF-C colocalized with F4/80^{+} cells, indicating that macrophages produce VEGF-C (Figure 4B).

Transport of fatty acids through lacteals. We examined lymph transport *via* microscopy after an intragastric administration of the fluorescently labeled tracer long-chain fatty acid BODIPY C16. At 3 h post-administration, BODIPY staining of the jejunum in HFD-fed WT and RAMP1$^{-/-}$ mice was increased in the villi when compared with ND-fed WT and RAMP1$^{-/-}$ mice (Figure 5A). However, no statistically significant differences in the fluorescent area was observed between HFD-fed WT and RAMP1$^{-/-}$ mice (Figure 5B). By contrast, BODIPY fluorescence intensity in the circulation of HFD-fed RAMP1$^{-/-}$ mice was higher than that of HFD-fed WT mice (Figure 5C). These results suggest that HFD-fed RAMP1$^{-/-}$ mice exhibited acceleration of lipid transport through lacteals, but not of lipid absorption by the enterocytes.

Lacteal lymphatic EC junctions. Increased concentration of fluorescently labeled fatty acids in HFD-fed RAMP1$^{-/-}$ mice may suggest hyperfunction of lacteals. Lipids are transported through lacteals, which are lined by lymphatic ECs forming button- and zipper-like junctions (25). Therefore, we determined the morphology of VE-cadherin+ lymphatic EC junctional patterns in WT and RAMP1$^{-/-}$ mice whole-mount intestines. In WT mice fed ND, the lacteals presented with both open and closed lymphatic EC junctions. This button-to-zipper pattern in the lacteals from RAMP1$^{-/-}$ mice fed on a ND appeared to be same as that from WT mice fed a ND. The proportion of zipper-like junctions was relatively increased in HFD-fed WT mice, while the proportion of button-like junctions was increased in HFD-fed RAMP1$^{-/-}$ mice (Figure 6A). These findings suggest that RAMP1 deletion increased button-like junctions in lacteals and facilitated lipid absorption and lymphatic transport, leading to their circulation into the bloodstream. As VEGF-A/VEGFR2 signaling has been suggested to be involved in zippering lacteals (26), we determined the gene expression levels of *Vegfa*, *Vegfr1*, and *Vegfr2* in the intestine (Figure 6B). The gene expression levels of *Vegfa* and *Vegfr2* in HFD-fed WT mice were higher than those in HFD-fed RAMP1$^{-/-}$ mice, while no statistically significant differences in *Vegfr1* mRNA levels between HFD-fed WT and RAMP1$^{-/-}$ mice were noted.

Discussion

Lacteals, specialized lymphatic vessels in the small intestine, play a critical role in absorbing dietary lipids and transporting them into the circulation (5). Our data showed that RAMP1$^{-/-}$ mice fed a HFD exhibited exacerbated obesity accompanied by increased levels of adipose tissue weights and lipids in the blood as compared with HFD-fed WT mice. HFD-fed RAMP1$^{-/-}$ mice displayed shorter and wider lacteals and lower expression of the pro-lymphangiogenic

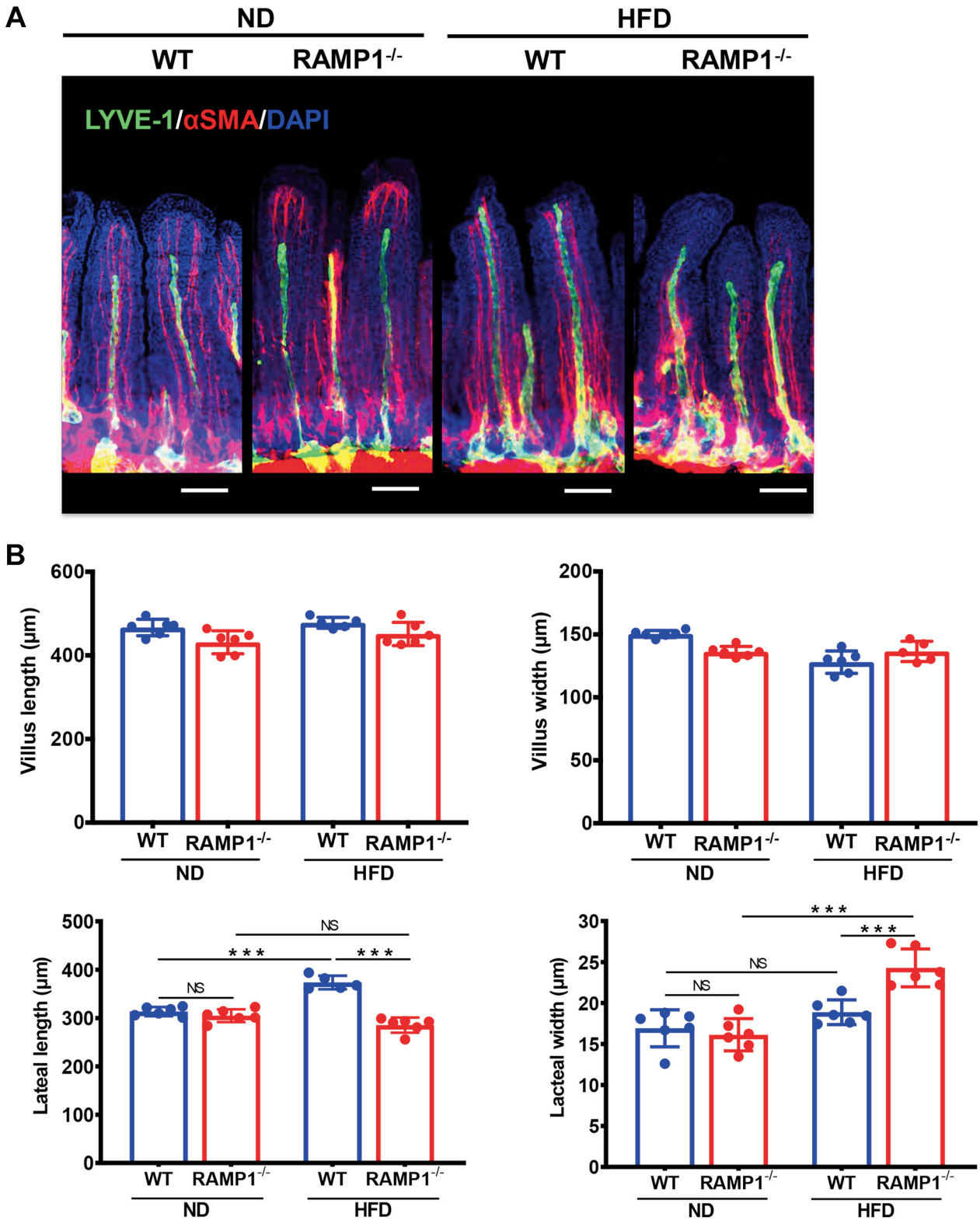

Figure 2. *Lacteals in wild type (WT) and RAMP1$^{-/-}$ mice after feeding of normal diet (ND) or high-fat diet (HFD). (A) Immunofluorescence staining for LYVE-1 (green) and αSMA (red) in the jejunum from WT and RAMP1$^{-/-}$ mice after feeding ND or HFD. Cell nuclei were stained with DAPI (blue). Scale bar: 100 μm. (B) The length and width of villi and lacteals from WT and RAMP1$^{-/-}$ mice after feeding ND or HFD. Data are expressed as the mean±SD. ***p<0.001; NS: Not significant.*

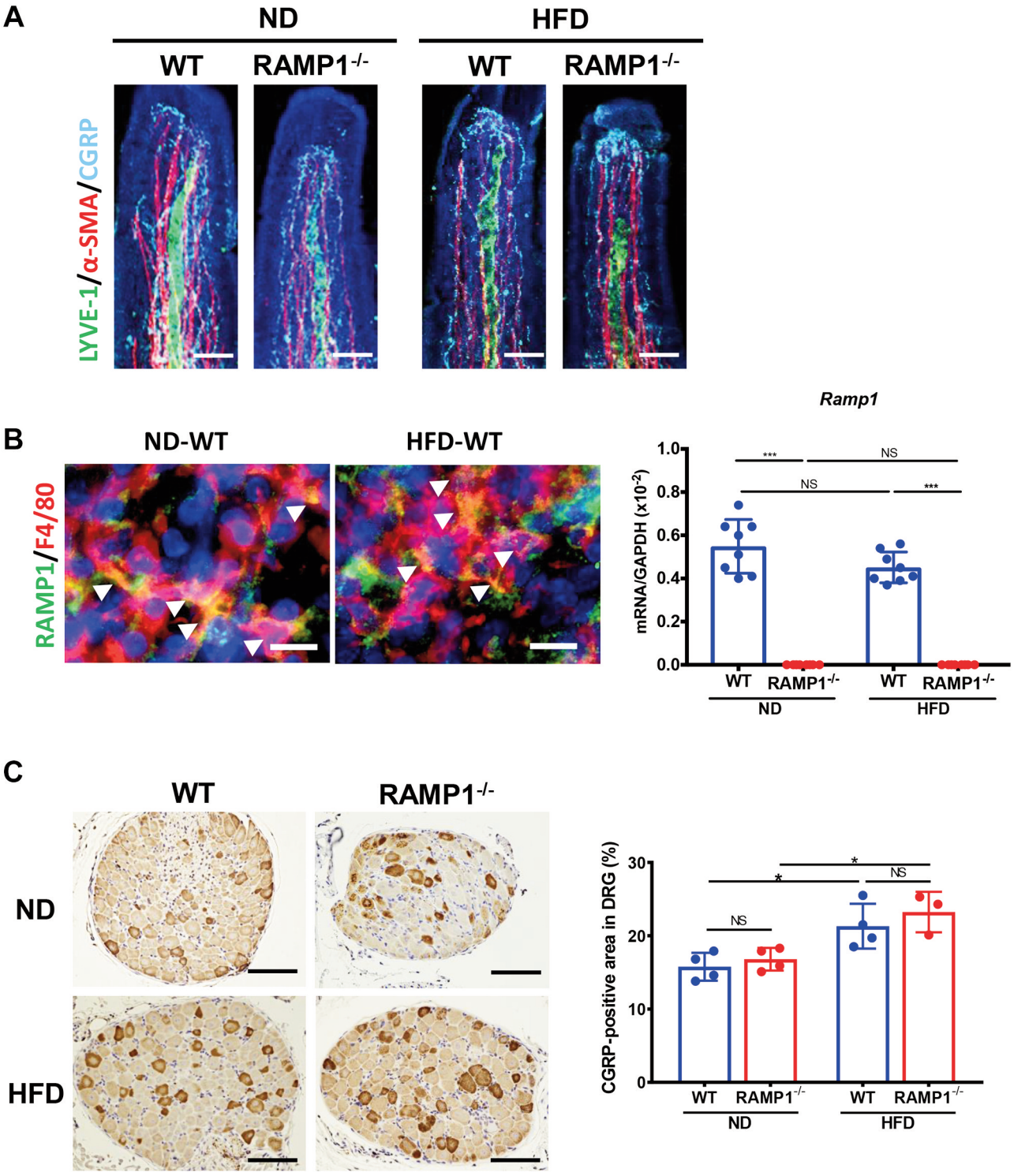

Figure 3. *Expression of CGRP and RAMP1. (A) Immunofluorescence staining for LYVE-1 (green), α-SMA (red), and CGRP (cyane) in the lacteals from wild type (WT) and RAMP1$^{-/-}$ mice after feeding normal diet (ND) or high-fat diet (HFD). Cell nuclei were stained with DAPI (blue). Scale bar: 50 μm. (B) Immunofluorescence staining for RAMP1 (green) and F4/80 (red) in the lacteals from WT mice after feeding ND or HFD. Cell nuclei were stained with DAPI (blue). Arrowheads indicate merged cells. Scale bar: 10 μm. The mRNA expression levels of Ramp1 in the jejunum from WT and RAMP1$^{-/-}$ mice fed with ND or HFD. Data are expressed as the mean±SD. ***p<0.001. NS: Not significant. (C) Immunostaining for CGRP in thoracic DRGs from WT and RAMP1$^{-/-}$ mice fed ND or HFD. Scale bar: 100 μm. The percentage of CGRP^{+} nerve cell area in the thoracic DRGs. Data are expressed as the mean±SD. *p<0.05; NS: Not significant.*

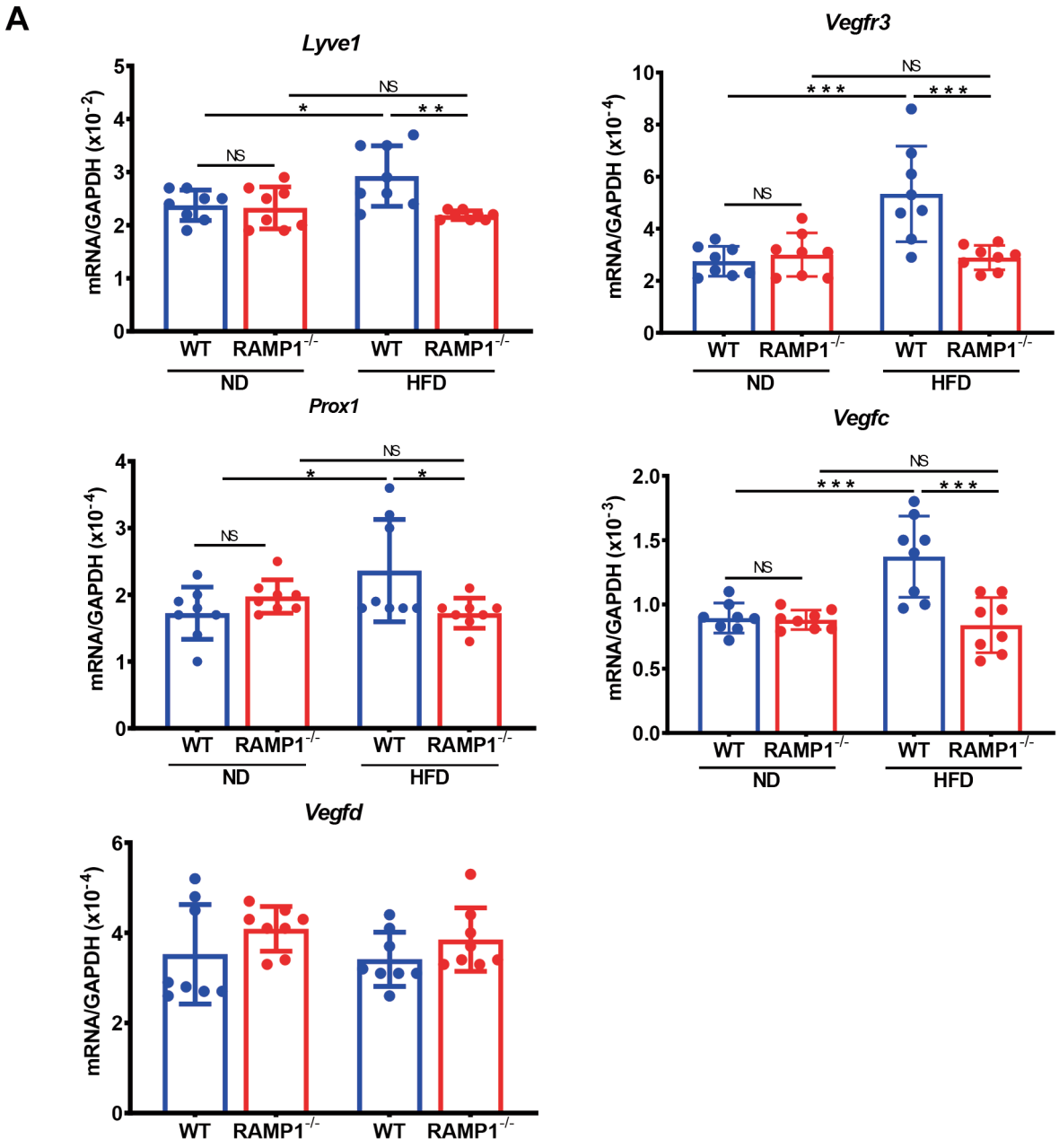

Figure 4. *Continued*

promoting cytokine VEGF-C and of lymphatic EC-related genes including *Lyve-1, Vegfr-3, and Prox1* than HFD-fed WT mice. However, the lipid concentration in the blood of HFD-fed RAMP1$^{-/-}$ mice was higher than that in the blood of HFD-fed WT mice. Increased proportions of button-like junctions and decreased proportions of zipper-like junctions were observed in lacteals from HFD-fed RAMP1$^{-/-}$ mice. In contrast, increased zipper-like junctions and decreased button-like junctions were observed in HFD-fed WT mice. These results suggest that the deletion of RAMP1 signaling was involved in diet-induced obesity by increasing the transport of absorbed lipids predominantly *via* button-like junctions in widened lacteals.

The present results demonstrated that RAMP1$^{-/-}$ mice exhibited enhanced diet-induced obesity accompanied by systemic metabolic consequences, indicating that deletion of RAMP1 signaling would enhance diet-induced obesity. As dietary lipids are absorbed by the small intestinal villi, we

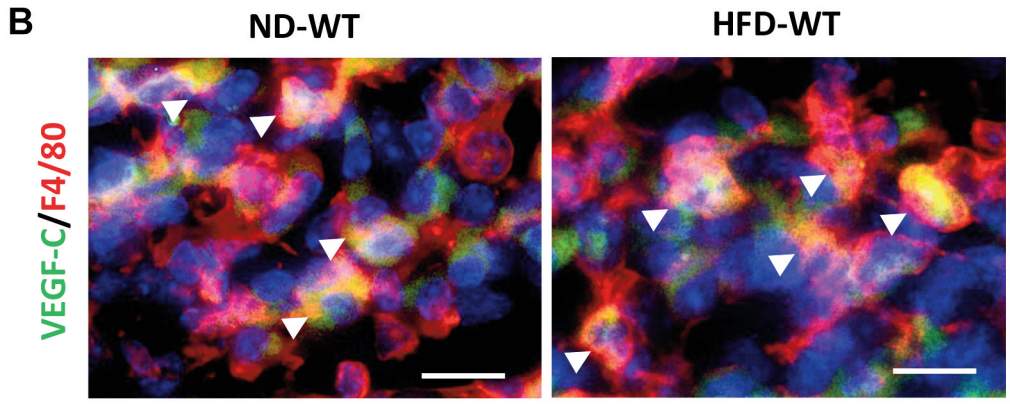

Figure 4. *Expression of lymphatic EC and pro-lymphangiogenic cytokines in wild type (WT) and RAMP1$^{-/-}$ mice after feeding normal diet (ND) or high-fat diet (HFD). (A) mRNA expression levels of Vegfr3, Prox1, Lyve-1, Vegfc, and Vegfd in the jejunum from WT and RAMP1$^{-/-}$ mice fed ND or HFD. Data are expressed as the mean±SD. *p<0.05, **p<0.01, and ***p<0.001; NS: Not significant. (B) Immunofluorescence staining for VEGF-C (green) and F4/80 (red) in the lacteals from WT mice after feeding ND or HFD. Cell nuclei were stained with DAPI (blue). Arrowheads indicate merged cells. Scale bar: 10 μm.*

evaluated the intestinal expression of CGRP and RAMP1 in mice fed ND or HFD. CGRP^{+} nerve fibers were diffusely distributed in the intestinal villi, where they surrounded the lacteals and were parallel to the smooth muscle fibers. However, the magnitude of the distribution did not appear to differ between the two genotypes fed the ND or HFD. In contrast, others (27) have demonstrated that RAMP1$^{-/-}$ mice fed a ND show decreased density of tyrosine hydroxylase-labeled nerves surrounding the villus lacteals. The discrepancies between the two studies might have arisen from the use of different nerve markers (catecholamine nerve fibers *vs*. sensory nerve fibers) for analysis. Because CGRP is generated in the DRG, we compared CGRP during the feeding of ND or HFD in WT and RAMP1$^{-/-}$ mice. When compared to mice-fed ND, CGRP expression was up-regulated after HFD feeding in both genotypes of mice; however, no statistically significant differences were found between the two groups. These results indicate that both WT and RAMP1$^{-/-}$ mice displayed CGRP production in the DRG to a similar extent in response to HFD feeding.

VEGF-C is a potent activator of lymphatic vessel growth through VEGFR-3 signaling (28). Accumulating evidence suggests that VEGF-C plays an important role in maintaining lacteal integrity (10, 11, 24, 25). Inactivation of VEGFR3 reduces VEGF-C levels and lacteal length (11, 12). Based on these findings, we determined the expression levels of lymphatic EC-related genes, including *Lyve-1, Vegfr-3,* and *Prox1*, in the jejunum. The mRNA levels of lymphatic EC-related genes in HFD-fed WT mice were higher than those in ND-fed WT and RAMP1$^{-/-}$ mice, whereas those in HFD-fed RAMP1$^{-/-}$ mice were lower than those in HFD-fed WT mice. The same was true for the expression of *Vegfc*, a pro-lymphangiogenic cytokine; however, no statistically significant difference in *Vegfd* mRNA expression was observed between the groups. These results indicate that short lacteal lengths in RAMP1$^{-/-}$ mice fed a HFD were accompanied by reduced expression of VEGF-C and VEGFR3. Thus, inhibiting RAMP1 signaling may reduce the expression levels of lymphatic EC-related genes and those of a pro-lymphangiogenic promoting cytokine during HFD feeding, resulting in the suppression of lacteal growth in response to HFD. In addition to the lacteal length, the width of lacteals in RAMP1$^{-/-}$ mice fed a HFD was higher than that in WT mice fed a HFD, which is consistent with the results of previous studies (27). Because the VEGF-C/VEGFR3 pathway is suggested to be involved in regulating the width of lacteals (11, 25), dilation of lacteals in HFD-fed RAMP1$^{-/-}$ mice is likely mediated by the reduced expression of VEGF-C and VEGFR3. Further work is required to understand the underlying mechanisms by which the deletion of RAMP1 signaling results in lacteal the dilation during HFD feeding.

Previously, we have shown that RAMP1 signaling in cultured bone marrow-derived macrophages is involved in the production of VEGF-C (19, 23). In the present study, we demonstrated that F4/80^{+} macrophages adjacent to lacteals expressed VEGF-C, which is consistent with other results indicating that macrophages are a source of VEGF-C (12). In addition, longitudinal SMCs surrounding the lacteals have been shown to be sources of VEGF-C (11). VEGF-C contributes not only to intestinal lymphatic maintenance but also to lipid absorption. VEGF-C deletion in mice prevents lacteal growth and attenuates lipid absorption. Additionally, the inhibition of VEGFR3 signaling decreases lipid absorption and transport, thereby contributing to the suppression of diet-induced obesity (29, 30). Although the present study demonstrated that HFD-fed

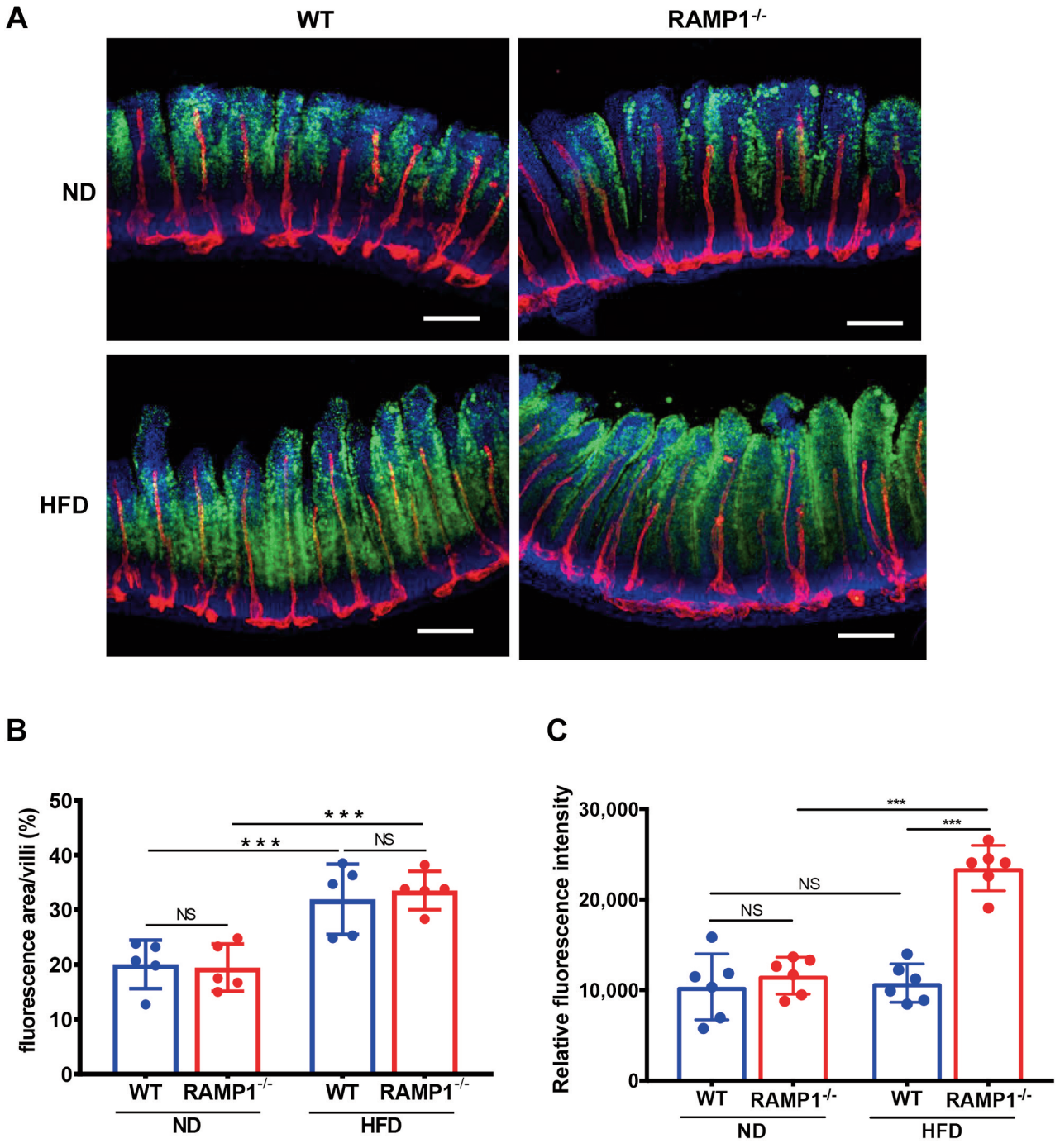

Figure 5. *Uptake of a fluorescent fatty acid in the intestinal villi and circulation at 3 h after oral administration. (A) Representative images of uptake of the fluorescent long-chain fatty acid tracer BODIPY C16 in intestinal villi of wild type (WT) and RAMP1$^{-/-}$ mice. Scale bars, 100 μm. (B) Percentage of fluorescence area in the intestinal villi. Data are expressed as the mean±SD from 5 villi in each animal. ***p<0.001; NS: not significant. (C) Fluorescence intensity in the circulation. Data are expressed as the mean±SD. ***p<0.001. NS: Not significant.*

RAMP1$^{-/-}$ mice exhibited decreased mRNA levels of *Vegfc* and *Vegfr3* and suppressed lacteal development, as indicated by shortened lacteal length and enlarged lacteal width, HFD-fed RAMP1$^{-/-}$ mice did not show impaired lipid absorption and transport. Rather, our data indicated that the deletion of RAMP1 signaling in HFD-fed mice

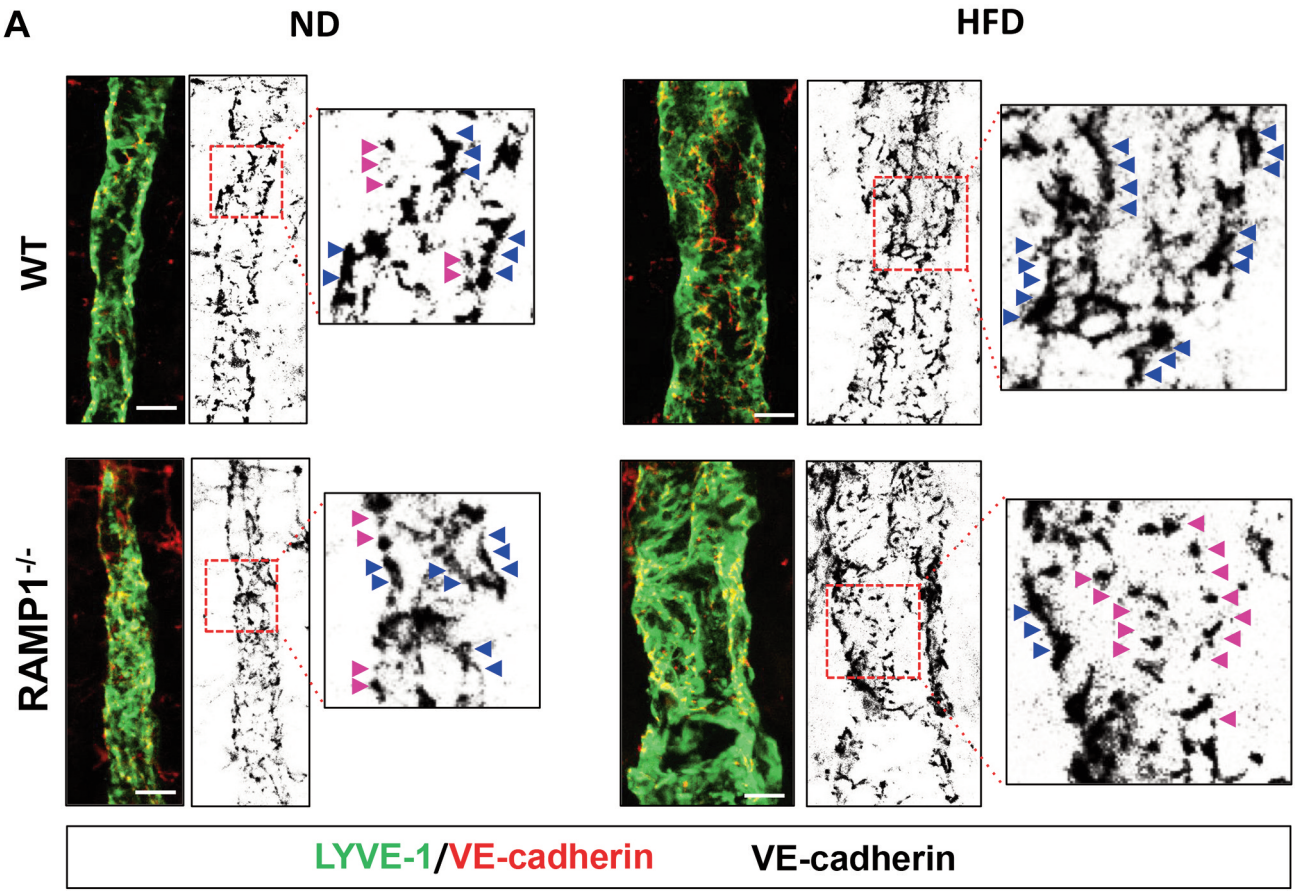

Figure 6. *Button and zipper junctions in lacteals and expression of VEGF-A and its receptors from wild type (WT) and RAMP1$^{-/-}$ mice. (A) Representative images of VE-cadherin^{+} (red) junctions of LYVE-1^{+} (green) lacteals in WT and RAMP1$^{-/-}$ mice fed ND or HFD. Red dashed box in the right panel indicates VE-cadherin^{+} (black) lymphatic EC junctions in lacteals of jejunum. Button-like (red arrowheads) and zipper-like (blue arrowheads) junctions. Right panel is a high-magnification image of the area outlined by the white dashed box. Scale bar: 10 μm. (B) mRNA expression levels of Vegfa, Vegfr1, and Vegfr2 in the jejunum from WT and RAMP1$^{-/-}$ mice fed ND or HFD. Data are expressed as the mean±SD. *p<0.05 and ***p<0.001; NS: Not significant.*

stimulated absorption of an orally administered fluorescent lipid tracer *via* lacteals, which led to increased serum levels of cholesterol and triglycerides. These results suggest that factors other than decreased levels of VEGF-C and VEGFR3 expression contribute to increased lipid uptake and transport in HFD-fed RAMP1$^{-/-}$ mice.

Cell–cell junctions are essential components of the lacteal structure and function. Lymphatic ECs are connected by functionally specialized junctions such as VE-cadherin. Lymphatic ECs in the initial lymphatics are interconnected by discontinuous button-like junctions, while the downstream collecting lymphatics exhibit continuous zipper-like junctions located at the cell borders with no openings (3). It is known that the button-like junctions in the initial lymphatics permit easy access of large molecules to the lymphatic vasculature, whereas zipper-like junctions prevent their entry into the lymphatic vessels (31). Regarding the villi of lymphatic vessels and lacteals, zippering of the lacteals inhibits uptake of chylomicron and renders mice resistant to diet-induced obesity (26). Lymphatic vessels with button-like junctions drain into the lymphatic system faster than lymphatic vessels with zipper-like junctions (32). In addition to the enlargement of lacteals, HFD-fed RAMP1$^{-/-}$ mice displayed an increase in the proportion of discontinuous button-like junctions, whereas continuous zipper-like junctions were predominant in HFD-fed WT mice. Thus, the deletion of RAMP1 signaling may increase the discontinuous-shaped junctions in lacteals. Consistent with this observation, when a fluorescent lipid tracer was orally administered, we observed an increase in fluorescence levels in HFD-fed RAMP1$^{-/-}$ mice as compared to those in HFD-fed WT mice. These results suggest that the presence of more discontinuous junctions in the lacteals from HFD-fed RAMP1$^{-/-}$ mice may increasingly permit transport of dietary lipids into the lacteals to promote lymph transport of dietary lipids to the circulation.

Uptake of chylomicron *via* lacteals is regulated by dynamic changes in cell–cell junctions through VEGF-A/VEGFR-2 signaling pathway. Zippering of the lacteal junctions suppresses chylomicron uptake and prevents diet-induced obesity in mice (26). High levels of VEGF-A induce lymphatic ECs in lacteals to form zipper-like junctions, thereby preventing chylomicron passage (26, 33). As stated above, the current study suggested that the predominant appearance of button-like junctions in HFD-fed RAMP1$^{-/-}$ mice might allowed the entry of more lipids into the lacteals than the predominant appearance of zipper-like junctions in HFD-fed WT mice. The present study also revealed upregulated expressions of VEGF-A and VEGFR2 in the small intestine of HFD-fed WT mice compared to HFD-fed RAMP1$^{-/-}$ mice, suggesting that VEGF-A/VEGFR2-induced lacteal zippering *via* RAMP1 signaling in WT mice inhibits the excessive uptake of dietary lipids. Further studies are needed to examine whether RAMP1 signaling contributes to the transition from buttons to zipper junctions in lacteals by enhancing the VEGF-A/VEGFR2 pathway under conditions of suppressed bioavailability of VEGFR1.

Enteric neurons are closely associated with lacteals. Our data demonstrated that CGRP nerve fibers are abundantly distributed in the intestinal villi. CGRP nerve fibers surround lacteals and SMCs. Furthermore, *in vivo* microscopic studies have demonstrated that lacteals do not simply act as passive conduits; instead, longitudinal SMCs surrounding the lacteals promote the drainage of absorbed fat by actively contracting and squeezing adjacent lacteals in response to the autonomic nervous system (34). As CGRP negatively regulates the movement of gastric SMCs (35), it is likely that inhibiting RAMP1 signaling in SMCs is involved in active contraction of lacteals, leading to the promotion of the transport of absorbed dietary fats. The precise interaction between RAMP1 signaling and SMCs along lacteals during HFD feeding remains to be elucidated.

The current study has several limitations. First, our study lacks data on food intake and energy expenditure from RAMP1$^{-/-}$ and WT mice. It is reported that the CGRP/RAMP1 signaling pathway promotes food intake and energy expenditure, which would induce obesity (36, 37). Second, the present results do not include any information from obese patients.

Conclusion

This study demonstrated that HFD-induced obesity in RAMP1$^{-/-}$ mice resulted in suppressed lymphatic vessel growth as indicated by decreased levels of lymphatic vessel markers, including VEGFR3, LYVE-1, and Prox1, which are critical lymphangiogenesis reporters on lymphatic ECs, as well as pro-lymphatic stimulating factors, including VEGF-C. Deletion of RAMP1 signaling stimulates uptake and transport of dietary fats through the discontinuous junctions of lacteals, which would lead to excessive obesity. Specific activation of RAMP1 signaling may represent a target for the therapeutic management of diet-induced obesity and metabolic disorders through regulation of lipid transport by lacteals.

Conflicts of Interest

The Authors declare that there are no conflicts of interest in relation to this study.

Authors' Contributions

KH conceived, designed, and performed experiments, collected the data, analyzed the data, and wrote the manuscript. AY, MT, and YI performed experiments and data collection, and provided technical support. MM verified the experimental results and analyzed the data. KT provided the transgenic mice and helped to design the experimental protocols. HA analyzed the experimental data and revised the manuscript.

Acknowledgements

The Authors thank Michiko Ogino and Kyoko Yoshikawa for technical assistance. This work was supported by Grants from the Japanese Ministry of Education, Culture, Sports, Science, and Technology

(MEXT) (22K06651 to KH and 22K08856 to YI), the Takeda Science Foundation (to KH), and a Project Research Grant from the Graduate School of Medical Sciences, Kitasato University (to KH).

References

1 Oliver G, Kipnis J, Randolph GJ, Harvey NL: The lymphatic vasculature in the 21(st) century: Novel functional roles in homeostasis and disease. Cell 182(2): 270-296, 2020. DOI: 10.1016/j.cell.2020.06.039

2 Xiao C, Stahel P, Carreiro AL, Buhman KK, Lewis GF: Recent advances in triacylglycerol mobilization by the gut. Trends Endocrinol Metab 29(3): 151-163, 2018. DOI: 10.1016/j.tem.2017.12.001

3 Cifarelli V, Eichmann A: The intestinal lymphatic system: Functions and metabolic implications. Cell Mol Gastroenterol Hepatol 7(3): 503-513, 2019. DOI: 10.1016/j.jcmgh.2018.12.002

4 Savetsky IL, Albano NJ, Cuzzone DA, Gardenier JC, Torrisi JS, García Nores GD, Nitti MD, Hespe GE, Nelson TS, Kataru RP, Dixon JB, Mehrara BJ: Lymphatic function regulates contact hypersensitivity dermatitis in obesity. J Invest Dermatol 135(11): 2742-2752, 2015. DOI: 10.1038/jid.2015.283

5 Jiang X, Tian W, Nicolls MR, Rockson SG: The lymphatic system in obesity, insulin resistance, and cardiovascular diseases. Front Physiol 10: 1402, 2019. DOI: 10.3389/fphys.2019.01402

6 Henry L, Paik J, Younossi ZM: Review article: the epidemiologic burden of non-alcoholic fatty liver disease across the world. Aliment Pharmacol Ther 56(6): 942-956, 2022. DOI: 10.1111/apt.17158

7 Harvey NL, Srinivasan RS, Dillard ME, Johnson NC, Witte MH, Boyd K, Sleeman MW, Oliver G: Lymphatic vascular defects promoted by Prox1 haploinsufficiency cause adult-onset obesity. Nat Genet 37(10): 1072-1081, 2005. DOI: 10.1038/ng1642

8 Escobedo N, Proulx ST, Karaman S, Dillard ME, Johnson N, Detmar M, Oliver G: Restoration of lymphatic function rescues obesity in Prox1-haploinsufficient mice. JCI Insight 1(2): e85096, 2016. DOI: 10.1172/jci.insight.85096

9 Karkkainen MJ, Saaristo A, Jussila L, Karila KA, Lawrence EC, Pajusola K, Bueler H, Eichmann A, Kauppinen R, Kettunen MI, Yla-Herttuala S, Finegold DN, Ferrell RE, Alitalo K: A model for gene therapy of human hereditary lymphedema. Proc Natl Acad Sci U.S.A. 98(22): 12677-12682, 2001. DOI: 10.1073/pnas.221449198

10 Bernier-Latmani J, Petrova TV: Intestinal lymphatic vasculature: structure, mechanisms and functions. Nat Rev Gastroenterol Hepatol 14(9): 510-526, 2017. DOI: 10.1038/nrgastro.2017.79

11 Nurmi H, Saharinen P, Zarkada G, Zheng W, Robciuc MR, Alitalo K: VEGF-C is required for intestinal lymphatic vessel maintenance and lipid absorption. EMBO Mol Med 7(11): 1418-1425, 2015. DOI: 10.15252/emmm.201505731

12 Suh SH, Choe K, Hong SP, Jeong SH, Mäkinen T, Kim KS, Alitalo K, Surh CD, Koh GY, Song JH: Gut microbiota regulates lacteal integrity by inducing VEGF-C in intestinal villus macrophages. EMBO Rep 20(4): e46927, 2019. DOI: 10.15252/embr.201846927

13 Ohno T, Hattori Y, Komine R, Ae T, Mizuguchi S, Arai K, Saeki T, Suzuki T, Hosono K, Hayashi I, Oh-Hashi Y, Kurihara Y, Kurihara H, Amagase K, Okabe S, Saigenji K, Majima M: Roles of calcitonin gene-related peptide in maintenance of gastric mucosal integrity and in enhancement of ulcer healing and angiogenesis. Gastroenterology 134(1): 215-225, 2008. DOI: 10.1053/j.gastro.2007.10.001

14 Ichikawa S, Kasahara D, Iwanaga T, Uchino S, Fujita T: Peptidergic nerve terminals associated with the central lacteal lymphatics in the ileal villi of dogs. Arch Histol Cytol 54(3): 311-320, 1991. DOI: 10.1679/aohc.54.311

15 Poole DP, Lee M, Tso P, Bunnett NW, Yo SJ, Lieu T, Shiu A, Wang JC, Nomura DK, Aponte GW: Feeding-dependent activation of enteric cells and sensory neurons by lymphatic fluid: evidence for a neurolymphocrine system. Am J Physiol Gastrointest Liver Physiol 306(8): G686-G698, 2014. DOI: 10.1152/ajpgi.00433.2013

16 Hay DL, Christopoulos G, Christopoulos A, Poyner DR, Sexton PM: Pharmacological discrimination of calcitonin receptor: Receptor activity-modifying protein complexes. Mol Pharmacol 67(5): 1655-1665, 2005. DOI: 10.1124/mol.104.008615

17 Majima M, Ito Y, Hosono K, Amano H: CGRP/CGRP receptor antibodies: Potential adverse effects due to blockade of neovascularization? Trends Pharmacol Sci 40(1): 11-21, 2019. DOI: 10.1016/j.tips.2018.11.003

18 Kurashige C, Hosono K, Matsuda H, Tsujikawa K, Okamoto H, Majima M: Roles of receptor activity-modifying protein 1 in angiogenesis and lymphangiogenesis during skin wound healing in mice. FASEB J 28(3): 1237-1247, 2014. DOI: 10.1096/fj.13-238998

19 Honda M, Ito Y, Hattori K, Hosono K, Sekiguchi K, Tsujikawa K, Unno N, Majima M: Inhibition of receptor activity-modifying protein 1 suppresses the development of endometriosis and the formation of blood and lymphatic vessels. J Cell Mol Med 24(20): 11984-11997, 2020. DOI: 10.1111/jcmm.15823

20 Mishima T, Ito Y, Nishizawa N, Amano H, Tsujikawa K, Miyaji K, Watanabe M, Majima M: RAMP1 signaling improves lymphedema and promotes lymphangiogenesis in mice. J Surg Res 219: 50-60, 2017. DOI: 10.1016/j.jss.2017.05.124

21 Tsujikawa K, Yayama K, Hayashi T, Matsushita H, Yamaguchi T, Shigeno T, Ogitani Y, Hirayama M, Kato T, Fukada S, Takatori S, Kawasaki H, Okamoto H, Ikawa M, Okabe M, Yamamoto H: Hypertension and dysregulated proinflammatory cytokine production in receptor activity-modifying protein 1-deficient mice. Proc Natl Acad Sci U S A 104(42): 16702-16707, 2007. DOI: 10.1073/pnas.0705974104

22 Karaman S, Hollmén M, Robciuc MR, Alitalo A, Nurmi H, Morf B, Buschle D, Alkan HF, Ochsenbein AM, Alitalo K, Wolfrum C, Detmar M: Blockade of VEGF-C and VEGF-D modulates adipose tissue inflammation and improves metabolic parameters under high-fat diet. Mol Metab 4(2): 93-105, 2014. DOI: 10.1016/j.molmet.2014.11.006

23 Tsuru S, Ito Y, Matsuda H, Hosono K, Inoue T, Nakamoto S, Kurashige C, Mishima T, Tsujikawa K, Okamoto H, Majima M: RAMP1 signaling in immune cells regulates inflammation-associated lymphangiogenesis. Lab Invest 100(5): 738-750, 2020. DOI: 10.1038/s41374-019-0364-0

24 Hong SP, Yang MJ, Cho H, Park I, Bae H, Choe K, Suh SH, Adams RH, Alitalo K, Lim D, Koh GY: Distinct fibroblast subsets regulate lacteal integrity through YAP/TAZ-induced VEGF-C in intestinal villi. Nat Commun 11(1): 4102, 2020. DOI: 10.1038/s41467-020-17886-y

25 Petrova TV, Koh GY: Biological functions of lymphatic vessels. Science 369(6500): eaax4063, 2020. DOI: 10.1126/science.aax4063

26 Zhang F, Zarkada G, Han J, Li J, Dubrac A, Ola R, Genet G, Boyé K, Michon P, Künzel SE, Camporez JP, Singh AK, Fong GH, Simons M, Tso P, Fernández-Hernando C, Shulman GI, Sessa WC, Eichmann A: Lacteal junction zippering protects against diet-induced obesity. Science 361(6402): 599-603, 2018. DOI: 10.1126/science.aap9331

27 Davis RB, Ding S, Nielsen NR, Pawlak JB, Blakeney ES, Caron KM: Calcitonin-receptor-like receptor signaling governs intestinal lymphatic innervation and lipid uptake. ACS Pharmacol Transl Sci 2(2): 114-121, 2019. DOI: 10.1021/acsptsci.8b00061

28 Alitalo K: The lymphatic vasculature in disease. Nat Med 17(11): 1371-1380, 2011. DOI: 10.1038/nm.2545

29 Shew T, Wolins NE, Cifarelli V: VEGFR-3 signaling regulates triglyceride retention and absorption in the intestine. Front Physiol 9: 1783, 2018. DOI: 10.3389/fphys.2018.01783

30 Hokkanen K, Tirronen A, Ylä-Herttuala S: Intestinal lymphatic vessels and their role in chylomicron absorption and lipid homeostasis. Curr Opin Lipidol 30(5): 370-376, 2019. DOI: 10.1097/MOL.0000000000000626

31 Baluk P, Fuxe J, Hashizume H, Romano T, Lashnits E, Butz S, Vestweber D, Corada M, Molendini C, Dejana E, McDonald DM: Functionally specialized junctions between endothelial cells of lymphatic vessels. J Exp Med 204(10): 2349-2362, 2007. DOI: 10.1084/jem.20062596

32 Wu C, Li H, Zhang P, Tian C, Luo J, Zhang W, Bhandari S, Jin S, Hao Y: Lymphatic flow: a potential target in sepsis-associated acute lung injury. J Inflamm Res 13: 961-968, 2020. DOI: 10.2147/JIR.S284090

33 Churchill MJ, du Bois H, Heim TA, Mudianto T, Steele MM, Nolz JC, Lund AW: Infection-induced lymphatic zippering restricts fluid transport and viral dissemination from skin. J Exp Med 219(5): e20211830, 2022. DOI: 10.1084/jem.20211830

34 Choe K, Jang JY, Park I, Kim Y, Ahn S, Park DY, Hong YK, Alitalo K, Koh GY, Kim P: Intravital imaging of intestinal lacteals unveils lipid drainage through contractility. J Clin Invest 125(11): 4042-4052, 2015. DOI: 10.1172/JCI76509

35 Mizuguchi S, Ohno T, Hattori Y, Kamata K, Arai K, Saeki T, Saigenji K, Hayashi I, Kuribayashi Y, Majima M: Calcitonin gene-related peptide released by capsaicin suppresses myoelectrical activity of gastric smooth muscle. J Gastroenterol Hepatol 20(4): 611-618, 2005. DOI: 10.1111/j.1440-1746.2004.03764.x

36 Zhang Z, Liu X, Morgan DA, Kuburas A, Thedens DR, Russo AF, Rahmouni K: Neuronal receptor activity-modifying protein 1 promotes energy expenditure in mice. Diabetes 60(4): 1063-1071, 2011. DOI: 10.2337/db10-0692

37 Sanford D, Luong L, Gabalski A, Oh S, Vu JP, Pisegna JR, Germano P: An intraperitoneal treatment with calcitonin gene-related peptide (CGRP) regulates appetite, energy intake/expenditure, and metabolism. J Mol Neurosci 67(1): 28-37, 2019. DOI: 10.1007/s12031-018-1202-3

Received August 16, 2023
Revised September 12, 2023
Accepted September 13, 2023